Will the circle be unbroken: specific mutations in the yeast Sm protein ring expose a requirement for assembly factor Brr1, a homolog of Gemin2

BEATE SCHWER,[1] ALLEN J. ROTH,[1] and STEWART SHUMAN[2]

[1]Microbiology and Immunology Department, Weill Cornell Medical College, New York, New York 10065, USA
[2]Molecular Biology Program, Sloan-Kettering Institute, New York, New York 10065, USA

ABSTRACT

A seven-subunit Sm protein ring assembles around specific U-rich RNA segments of the U1, U2, U4, and U5 snRNPs that direct pre-mRNA splicing. Using human snRNP crystal structures to guide mutagenesis in *Saccharomyces cerevisiae*, we gained new insights into structure–function relationships of the SmD1 and SmD2 subunits. Of 18 conserved amino acids comprising their RNA-binding sites or intersubunit interfaces, only Arg88 in SmD1 and Arg97 in SmD2 were essential for growth. Tests for genetic interactions with non-Sm splicing factors identified benign mutations of SmD1 (*N37A*, *R88K*, *R93A*) and SmD2 (*R49A*, *N66A*, *R97K*, *D99A*) that were synthetically lethal with null alleles of U2 snRNP subunits Lea1 and/or Msl1. Tests of 264 pairwise combinations of SmD1 and SmD2 alleles with each other and with a collection of SmG, SmE, SmF, SmB, and SmD3 alleles revealed 92 instances of inter-Sm synthetic lethality. We leveraged the Sm mutant collection to illuminate the function of the yeast Sm assembly factor Brr1 and its relationship to the metazoan Sm assembly factor Gemin2. Mutations in the adjacent SmE (*K83A*), SmF (*K32A*, *F33A*, *R74K*), SmD2 (*R49A*, *N66A*, *E74A*, *R97K*, *D99A*), and SmD1 (*E18A*, *N37A*) subunits —but none in the SmG, SmD3, and SmB subunits—were synthetically lethal with *brr1*Δ. Using complementation of *brr1*Δ lethality in two Sm mutant backgrounds as an in vivo assay of Brr1 activity, we identified as essential an N-terminal segment of Brr1 (amino acids 24–47) corresponding to the Gemin2 α1 helix that interacts with SmF and a Brr1 C-terminal peptide (^{336}QKDLIE^{341}) that, in Gemin2, interacts with SmD2.

INTRODUCTION

Seven paralogous Sm proteins assemble into a ring that forms the core scaffold of the U1, U2, U4, and U5 small ribonuclear proteins (snRNPs) that orchestrate pre-mRNA splicing (van der Feltz et al. 2012; Kondo et al. 2015; Li et al. 2016). The conserved fold of each Sm subunit comprises a five-strand antiparallel β-sheet, embellished in some cases by additional secondary structure elements and/or unstructured C-terminal extensions of varying length. Prior to assembly of the ring, the Sm proteins self-organize as three heteromeric subcomplexes: SmD3-SmB, SmF–SmE–SmG, and SmD1–SmD2 (Kambach et al. 1999). The assembled Sm ring is stabilized by main-chain and side-chain contacts between neighboring Sm subunits and by interactions with the uridine-rich Sm site of the snRNA, which threads through the central hole of the ring so that individual RNA nucleobases are engaged sequentially (5′–3′) by the SmF, SmE, SmG, SmD3, SmB, SmD1, and SmD2 subunits (Supplemental Fig. S1A; Kondo et al. 2015; Li et al. 2016). The stereotypic Sm protein–RNA contacts are made by an amino acid "triad" whereby the planar nucleobase is sandwiched by an arginine or lysine side chain from the β4–β5 loop (which makes a π-cation stack on the nucleobase) and a side chain from the β2–β3 loop (often an aromatic group that forms a π stack on the nucleobase), while an asparagine side chain of the β2–β3 loop makes hydrogen bonds to the nucleobase edge.

Crystal structures of the human Sm ring and its RNA interface with U1 and U4 snRNAs are known (Kambach et al. 1999; Weber et al. 2010; Kondo et al. 2015; Li et al. 2016), and recent cryo-EM studies of splicing complexes are providing similar insights into the budding and fission yeast Sm rings (Hang et al. 2015; Nguyen et al. 2015; Galej et al. 2016; Wan et al. 2016a,b; Yan et al. 2016). We have married these advances in snRNP structural biology to the genetics of budding yeast to elucidate structure–function relationships

Corresponding authors: bschwer@med.cornell.edu, s-shuman@ski.mskcc.org

Article is online at http://www.rnajournal.org/cgi/doi/10.1261/rna.059881.116.

and genetic interactions of the essential Sm ring subunits SmF, SmE, SmG, SmD3, and SmB (Schwer and Shuman 2015; Schwer et al. 2016).

The results of a cumulative alanine scan of 36 conserved amino acids of these five proteins revealed that subtracting 35 of the RNA-binding or Sm–Sm interfacial side chains had no effect on yeast vegetative growth under laboratory conditions and only one mutation (*SMF R74A*) elicited a slow-growth phenotype (Supplemental Fig. S1B). Yet, for SmF, SmE, SmG, SmD3, and SmB, as for so many components of the *S. cerevisiae* spliceosome, the effects of perturbing protein–RNA and protein–protein interactions were masked in an otherwise wild-type genetic background because of inherent functional redundancies of the yeast splicing machine. Our survey of genetic interactions with multiple non-Sm splicing factors showed that mutations of SmG, SmE, SmF, SmD3, and SmB consistently elicited synthetic lethality in the absence of U2 snRNP subunits Lea1 and Msl1 (Schwer and Shuman 2015; Schwer et al. 2016). Sporadic synergies of specific Sm mutations were observed absent other early spliceosome components: Mud1, Nam8, Mud2, and TMG caps.

Analysis of 142 pairwise combinations of single SmG, SmE, SmF, SmB, and SmD3 RNA site mutations highlighted the built-in redundancies of the Sm ring, whereby subtracting RNA contacts of any one Sm subunit is tolerated but simultaneous mutation of the RNA binding sites of any two of the five Sm subunits tested was lethal in 45 instances (Schwer and Shuman 2015; Schwer et al. 2016). These results suggested that six of seven intact RNA binding sites in the Sm ring might suffice for in vivo function, but five sites may not.

Here we extended the structure-guided mutagenesis and synthetic genetic array analysis to the SmD2 and SmD1 subunits and thereby identified RNA-binding residues SmD2 Arg97 and SmD1 Arg88 as essential constituents of the yeast Sm ring. Thus, "one bad apple" (specifically SmD2 or SmD1) can spoil the whole bunch. Nonetheless, we identified a network of pairwise synthetic lethalities of SmD2 and SmD1 mutations with lesions in other Sm subunits, reinforcing the conclusion that two bad apples in the bunch are fatal. We also unveiled many SmD2 and SmD1 mutations as synthetically lethal with *lea1*Δ and *msl1*Δ.

We leveraged our extensive yeast Sm mutant collection to acquire new insights into the function of the putative Sm assembly factor Brr1, a yeast homolog of the metazoan Sm assembly factor Gemin2 (Noble and Guthrie 1996; Liu et al. 1997; Kroiss et al. 2008). Brr1 is inessential for vegetative growth of *S. cerevisiae*, suggesting that the yeast Sm ring can assemble on snRNAs without the aid of a Gemin2-like chaperone. Here we report that certain mutations in the adjacent SmE, SmF, SmD2, and SmD1 subunits (but none in the adjacent SmG, SmD3, and SmB subunits) are synthetically lethal with *brr1*Δ. We surmise that specific perturbations of the SmE-F-D2-D1 ring segment affect self-assembly and unmask a requirement for Brr1 to compensate for weakened Sm protein–RNA or Sm protein–protein interactions. These findings enable budding yeast as a model system for the study of chaperone-mediated Sm assembly and structure–function studies of Brr1.

RESULTS

Structure-guided mutagenesis of yeast SmD2

The 110-amino acid *S. cerevisiae* SmD2 protein and the 118-amino acid human SmD2 polypeptide align with 81 positions of side chain identity/similarity (Fig. 1A). The secondary structure elements of human SmD2 are indicated below the amino acid sequence in Figure 1A. The tertiary structure of human SmD2 in the U4 snRNP crystal (Li et al. 2016) and its contacts to the Sm site of the U4 snRNA are shown in Figure 2A, where, for the purpose of this study, the conserved amino acids are numbered according to their positions in yeast SmD2. The lysine-rich β3–β4 loop is disordered in human SmD2; the corresponding loop in yeast SmD2 is shorter by seven amino acids (Fig. 1A). The N-terminal 12 amino acids of human SmD2, of which nine are conserved in yeast SmD2, are disordered in the human U1 snRNP and U4 snRNP structures. To address the contributions of the N-terminal segment to yeast SmD2 function, we serially deleted 12 or 30 amino acids, as indicated by the arrows in Figure 1A. The wild-type and *SMD2-N*Δ alleles were placed on *CEN LEU2* plasmids under the control of the native *SMD2* promoter and tested by plasmid shuffle for complementation of a *smd2*Δ p[*CEN URA3 SMD2*] strain. The resulting *SMD2-N*Δ strains were viable after FOA selection. Whereas *SMD2-NΔ12* cells grew as well as wild-type *SMD2* cells on YPD agar at 20–37°C, *SMD2-NΔ30* cells displayed a tight temperature-sensitive growth defect, evinced by slow growth at 34°C (as gauged by colony size) and no growth at 37°C (Fig. 1B). We conclude that: (i) the disordered N-terminal leader peptide is dispensable for yeast SmD2 activity in vivo; and (ii) the glutamate-rich segment from amino acids 13–30 that includes the α1 helix is critical for SmD2 function at higher temperatures.

The SmD2 subunit captures a uridine nucleotide of the U RNA Sm site. As shown for the U4 snRNP (Fig. 2A), SmD2 side chain Asn64 (Asn66 in yeast SmD2) makes bidentate hydrogen bonds from Nδ and Oδ to the O4 and N3 atoms of the uracil nucleobase. SmD2 Arg102 (Arg97 in yeast SmD2) makes a π-cation stack on the uracil. SmD2 His62 (His64 in yeast SmD2) completes the sandwich on the other face of the uracil, while also making van der Waals contacts to an adenine base 5 nt upstream of the uracil. Additional RNA contacts of SmD2 conserved side chains are as follows. Arg61 (Arg63 in yeast) coordinates the 5′-phosphate of that upstream adenosine. Arg47 (Arg49 in yeast) makes a π-cation stack on the adenine 3′ of the uracil while also making hydrogen bonds to a downstream internucleotide phosphate and a ribose 2′-OH. Asn49 (Asn51 in yeast) makes a hydrogen

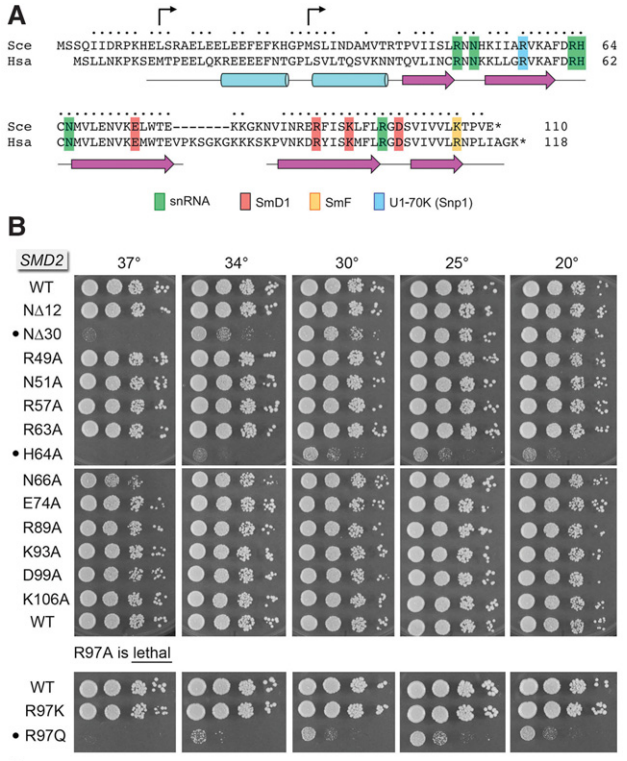

FIGURE 1. Structure-guided mutagenesis of SmD2. (*A*) Alignment of the primary structures of *S. cerevisiae* (Sce) and human (Hsa) SmD2. Positions of side chain identity/similarity are indicated by (•) *above* the yeast sequence. Gaps in the alignment are indicated by dashes. The secondary structure elements are depicted *below* the human sequence as magenta β strands (arrows) and cyan α helices (cylinders). Selected conserved SmD2 amino acids that make contacts to snRNA, flanking Sm ring subunits SmD1 or SmF, or U1 snRNP subunit U1-70K (Snp1 in yeast) are highlighted in color-coded boxes as indicated. *Forward* arrowheads indicate the first amino acids of the N-terminal truncations of yeast SmD2. (*B*) The wild-type and mutated *SMD2* alleles were tested for *smd2*Δ complementation by plasmid shuffle. The viable FOA-resistant *smd2*Δ strains bearing the indicated *SMD2* alleles were spot-tested for growth on YPD agar at the temperatures specified. Mutations that elicited a severe growth defect are indicated by (•). (*C*) Synthetic interactions of SmD2 mutants. Synthetically lethal pairs of alleles are highlighted in red boxes. Other negative pairwise interactions are classified as sick or very sick (yellow boxes) or temperature sensitive (*ts*) or cold sensitive (*cs*) (light green boxes). Gray boxes denote lack of mutational synergy.

bond to another distal ribose 2′-OH (Fig. 2A). The RNA-binding amino acids are shaded green in the sequence alignment in Figure 1A. SmD2 amino acids Glu72, Arg94, Lys98, and Asp104 (Glu74, Arg89, Lys93, and Asp99 in yeast; shaded orange in Fig. 1A) interact with the SmD1 subunit that flanks SmD2 in the ring. SmD2 residue Arg111 (Lys106 in yeast) contacts the neighboring SmF subunit. In the U1 snRNP, SmD2 Arg55 (Arg57 in yeast) contacts the U1-specific U1-70K subunit (Snp1 in yeast).

To interrogate the contributions of these snRNA and intersubunit contacts, we mutated yeast SmD2 residues Arg49, Asn51, Arg57, Arg63, His64, Asn66, Glu74, Arg89, Lys93, Arg97, Asp99, and Lys106 to alanine. The wild-type and *SMD2-Ala* alleles on *CEN LEU2* plasmids under the control of the native *SMD2* promoter were tested for *smd2*Δ complementation by plasmid shuffle. The *R97A* allele was uniquely lethal, i.e., no FOA-resistant colonies were obtained after 8 d of incubation at 20°C, 30°C, or 37°C. To examine

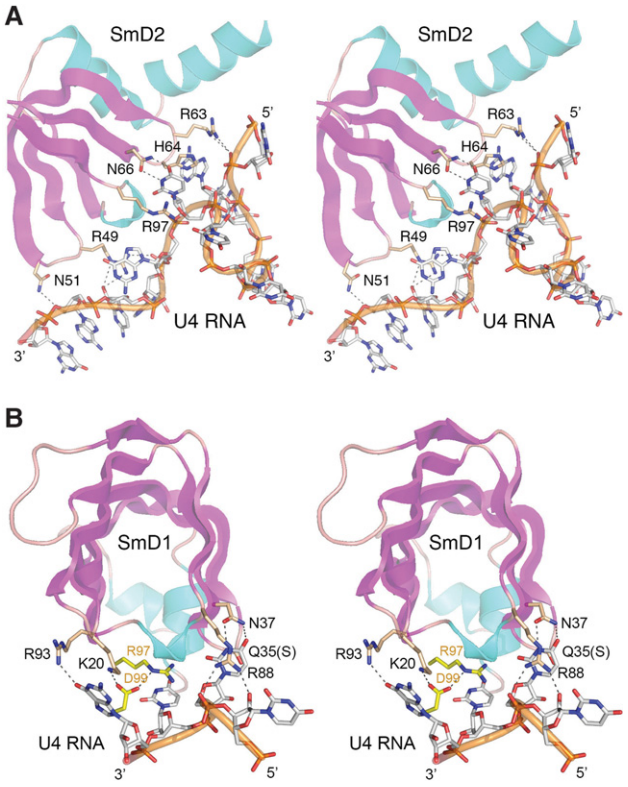

FIGURE 2. SmD2 and SmD1 structures and contacts with U4 snRNA. Stereo views of the human U4 snRNP structure highlighting the folds of SmD2 (panel *A*) and SmD1 (panel *B*)—depicted as cartoon traces with magenta β strands and cyan α helices—and their interactions with the Sm site in U4 snRNA (from pdb 4WZJ). Selected conserved amino acids are shown as stick models with beige carbons and numbered according to their positions in the yeast SmD2 and SmD1 polypeptides. (The counterpart of Gln35 in yeast SmD1 is Ser35 in human SmD1.) The U4 RNA is rendered as a stick model with gray carbons and a gold cartoon trace through the RNA phosphodiester backbone. Atomic contacts are indicated by dashed lines.

structure–activity relations at this essential RNA-binding arginine, we introduced conservative changes to lysine and glutamine and tested them for *smd2*Δ complementation. Whereas *R97K* cells grew as well as wild-type *SMD2* cells at all temperatures tested, the *R97Q* strain was extremely sick, i.e., it formed pinpoint colonies at 30°C–34°C and failed to grow at 37°C (Fig. 1B). Thus, we conclude that positive charge is the key essential property at position 97 of yeast SmD2.

The 11 other *SMD2-Ala* strains that survived FOA selection were tested for growth on YPD agar. The *H64A* strain was extremely sick, forming pinpoint colonies at 20°C–30°C and failing to thrive at 34°C–37°C (Fig. 1B), signifying the importance of this RNA-binding side chain for SmD2 function. *N66A* cells formed smaller colonies at 37°C, but the nine other *SMD2-Ala* strains thrived at 20–37°C (Fig. 1B), from which we conclude that none of these other RNA-binding or subunit-interacting side chains are essential per se for SmD2 activity in vivo.

Mutagenesis of yeast SmD1

The 146-amino acid *S. cerevisiae* SmD1 protein and the 119-amino acid human SmD1 polypeptide align with 67 positions of side chain identity/similarity (Fig. 3A). The secondary structure elements of human SmD1 from the N terminus to Asp82 (Asp109 in yeast) are indicated below the amino acid sequence in Figure 3A. Yeast SmD1 has a 27-amino acid segment inserted between the β3 and β4 strands that has no counterpart in human SmD1. Human and yeast SmD1 both have C-terminal extensions, but they are quite different in primary structure. The human SmD1 C terminus is composed of nine tandem Gly-Arg dipeptides that are absent in the yeast protein, although the yeast C terminus is enriched in basic amino acids. It is thought that the C termini of yeast and human SmD1 play a role in nuclear localization (Bordonné 2000; Girard et al. 2004).

To address the contributions of the C-terminal segment to SmD1 function, we serially truncated the polypeptide by 13, 27, and 40 amino acids, as indicated by the reverse arrows in Figure 3A. The wild-type and *SMD1-ΔC* alleles were placed on *CEN HIS3* plasmids under the control of the native *SMD1* promoter and tested by plasmid shuffle for complementation of a *smd1*Δ p[*CEN URA3 SMD1*] strain. The resulting *SMD1-ΔC* strains were viable after FOA selection and grew as well as wild-type *SMD1* cells on YPD agar (Fig. 3B). We conclude that the C-terminal segment distal to the α2 helix is dispensable for yeast SmD1 function in vivo. This accords with prior studies showing that a deletion of the C terminus of yeast SmD1 did not affect growth but was synthetically lethal with a deletion of the C-terminal segment of SmB (Bordonné 2000).

The tertiary structure of human SmD1 in the U4 snRNP crystal and its contacts to the Sm site of the U4 snRNA are shown in Figure 2B (with the conserved amino acids numbered according to their positions in yeast SmD1). SmD1 engages a uridine nucleotide of the U4 Sm site (specifically, the uridine immediately 5′ of the uridine bound by SmD2) via a Ser35–Asn37–Arg61 triad, the equivalent of which in yeast SmD1 is Gln35–Asn37–Arg88 (Figs. 2B, 3A). In addition, Arg66 (Arg93 in yeast) contacts a guanine 2 nt downstream from the uridine (Fig. 2B). Lys20 makes a salt bridge to SmD2 Asp104 (Asp99 in yeast SmD2); this SmD2 Asp in turn makes a salt bridge to the essential SmD2 arginine (Arg97 in yeast) (Fig. 2B). The aliphatic segment of the Lys20 side chain stacks on the guanine base engaged by SmD1 Arg93 (Fig. 2B). The crystal structure of human U1 snRNP (Kondo et al. 2015) reveals that SmD1 Glu18 makes

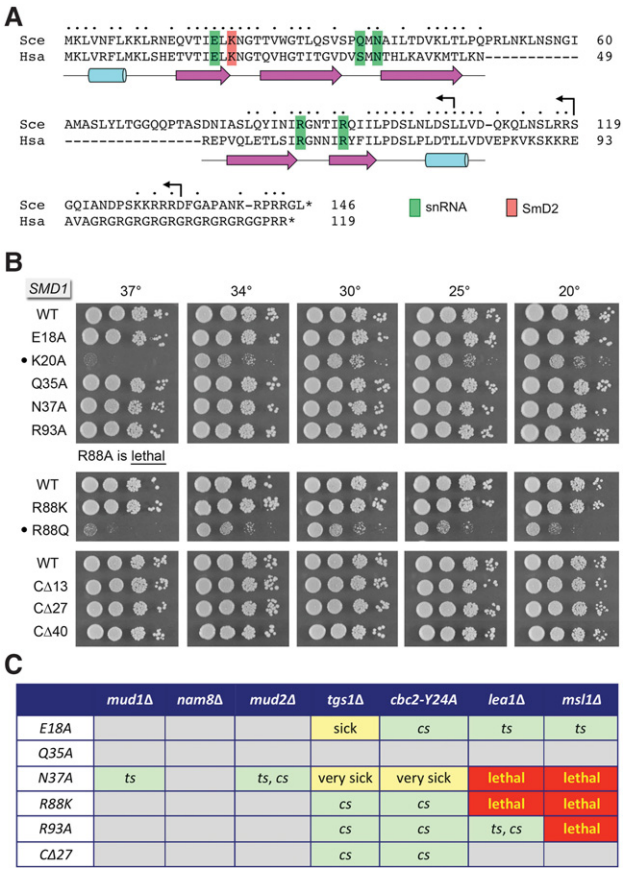

	mud1Δ	nam8Δ	mud2Δ	tgs1Δ	cbc2-Y24A	lea1Δ	msl1Δ
E18A				sick	cs	ts	ts
Q35A							
N37A	ts		ts, cs	very sick	very sick	lethal	lethal
R88K				cs	cs	lethal	lethal
R93A				cs	cs	ts, cs	lethal
CΔ27				cs	cs		

FIGURE 3. Mutagenesis of SmD1. (*A*) Alignment of the primary structures of *S. cerevisiae* (Sce) and human (Hsa) SmD1. Positions of side chain identity/similarity are indicated by (•) *above* the yeast sequence. Gaps in the alignment are indicated by dashes. The secondary structure elements are depicted *below* the human sequence as magenta β strands (arrows) and cyan α helices (cylinders). Selected conserved SmD1 amino acids that make contacts to snRNA or the flanking SmD2 subunit are highlighted in color-coded boxes as indicated. Reverse arrowheads indicate the last amino acids of the C-terminal truncations of yeast SmD1. (*B*) The wild-type and mutated *SMD1* alleles were tested for *smd1*Δ complementation by plasmid shuffle. The viable FOA-resistant *smd1*Δ strains bearing the indicated *SMD1* alleles were spot-tested for growth on YPD agar at the temperatures specified. (*C*) Synthetic interactions of SmD1 mutants. Synthetically lethal pairs of alleles are highlighted in red boxes. Other negative pairwise interactions are classified as sick or very sick (yellow boxes) or temperature sensitive (*ts*) or cold sensitive (*cs*) (light green boxes). Gray boxes denote lack of mutational synergy.

a salt bridge to SmD2 Arg94 (Arg89 in yeast SmD2) and also makes a hydrogen bond to the N2 atom of a guanine base in the U1 snRNA.

We performed an alanine scan of yeast SmD1 residues Glu18, Lys20, Gln35, Asn37, Arg88, and Arg93 and tested the *SMD1-Ala* alleles for *smd1*Δ complementation. The *R88A* allele was uniquely lethal. (Note that Arg88 in SmD1 is the counterpart of the essential Arg97 in SmD2.) The conservative *R88K* mutation restored SmD1 function, such that *R88K* cells grew as well as wild-type *SMD1* cells at all temperatures (Fig. 3B). In contrast, *R88Q* cells were slow growing at all temperatures tested (Fig. 3B). Thus, positive charge (enabling a π-cation stack on a uracil of the Sm site) is the key property at this position. Alanine mutations of putative SmD1 RNA-binding residues Gln35, Asn37, and Arg93, and of the RNA-binding/SmD2-interfacial residue Glu18 had no effect on cell growth at any temperature tested. Yet, the *K20A* mutation at the SmD2 interface elicited a tight *ts* defect at 37°C and slowed growth at lower temperatures (Fig. 3B).

Genetic interactions of SmD2 and SmD1 mutants with non-Sm splicing factors

To survey synthetic genetic interactions of biologically active mutations of conserved SmD2 and SmD1 amino acids at their RNA binding sites or subunit interfaces, we constructed a series of yeast strains in which the genes encoding inessential splicing factors Mud1, Nam8, Mud2, Tgs1, Lea1, or Msl1 were deleted in the *smd2*Δ p[*CEN URA3 SMD2*] and *smd1*Δ p[*CEN URA3 SMD1*] backgrounds, thereby allowing tests of synergy by plasmid shuffle. Mud1 (the homolog of human U1A) and Nam8 are subunits of the yeast U1 snRNP. Mud2 (the homolog of human U2AF65) is a subunit of the Msl5•Mud2 branchpoint binding protein. Lea1 (the homolog of human U2A′) and Msl1 (the homolog of human U2B″) are subunits of the yeast U2 snRNP. Tgs1 is the methyltransferase enzyme that converts a 7-methylguanosine RNA cap to a 2,2,7-trimethylguanosine (TMG) cap, which is a signature modification of the U1, U2, U4, and U5 snRNAs (Mouaikel et al. 2002; Hausmann et al. 2008). We also tested for genetic interactions with the *cbc2-Y24A* mutation in the cap-binding pocket of the yeast nuclear cap-binding complex (CBC) (Qiu et al. 2012).

The results of the synergy tests for *SMD2 and SMD1* mutants are tabulated in Figures 1C and 3C, respectively. We categorized growth phenotypes as follows. Synthetically lethal pairs of alleles were those that failed to survive on FOA medium at any temperature (red boxes). FOA-resistant Sm mutant strains that grew as well as the corresponding wild-type Sm strain on YPD agar at all temperatures tested were deemed to have no mutational synergy (gray boxes). FOA-resistant Sm mutant strains that grew as well as wild-type Sm on YPD agar at one or more of the temperatures (defined as permissive temperature), but grew poorly or failed to grow at temperatures above and/or below the permissive temperature were classified as *ts*, *cs*, or *ts*/*cs* (light green boxes). Sm mutant strains that grew slowly (small colonies) or very slowly (pinpoint colonies) at their best temperatures were designated as sick or very sick (yellow boxes).

The consistent trend was that many of the otherwise benign RNA-binding site mutations or subunit interface mutations were lethal or severely growth-defective in the absence of U2 snRNP subunits Lea1 and Msl1. These included: *SMD2* alleles *R49A*, *N66A*, *E74A*, *R89A*, *R97K*, and *D99A* (Fig. 1C); and *SMD1* alleles *N37A*, *R88K*, and *R93A* (Fig. 3C). In contrast, these same mutations elicited either no synergies or conditional growth phenotypes (temperature sensitive or cold sensitive) in the absence of U1 snRNP subunits Mud1 and Nam8 or the branchpoint-binding protein subunit Mud2 (Figs. 1C, 3C). (Spot tests of growth of the *SMD2* mutant collection in the *mud1*Δ background illustrating the conditional phenotypes are shown in Supplemental Figure S2.) The effects of these SmD2 and SmD1 mutations in the *tgs1*Δ and *cbc2-Y24A* backgrounds were similarly or slightly less severe than in the *lea1*Δ and *msl1*Δ strains, and uniformly more severe than their effects in the *mud1*Δ, *nam8*Δ, and *mud2*Δ contexts (Figs. 1C, 3C). For example: *SMD2 R49A* and *D99A*, which were synthetic lethal with *lea1*Δ and *msl1*Δ, were viable but *ts/cs* or very sick in the *tgs1*Δ and *cbc2-Y24A* strains; *SMD2 N66A* was synthetically lethal with *lea1*Δ, *msl1*Δ, and *cbc2-Y24A* yet was viable though very sick in the *tgs1*Δ background; and *SMD2 R97K* was synthetically lethal with *lea1*Δ, *msl1*Δ, and *tgs1*Δ yet was viable albeit very sick in the *cbc2-Y24A* strain (Fig. 1C). *SMD1* mutations *N37A*, *R88K*, and *R93A*, which were synthetically lethal with *msl1*Δ, were viable and either very sick (*N37A*) or cold sensitive (*R88K*, *R93A*) with *tgs1*Δ and *cbc2-Y24A* (Fig. 3C; see Supplemental Fig. S3 for spot tests of growth of the *SMD1* mutants in the *cbc2-Y24A* background). *SMD1* allele *CΔ27* was unique in displaying synergies (*cs*) with *tgs1*Δ and *cbc2-Y24A* but no synergies with *lea1*Δ and *msl1*Δ (Fig. 3C).

SmD1 mutations synergize with mutations in other Sm subunits

Analysis of 55 pairwise combinations of five benign SmD1 mutations (*E18A*, *Q35A*, *N37A*, *R88K*, *R93A*) with 11 benign mutations in SmD2 identified 16 instances of synthetic lethality, 28 mutant pairs that had no effect on yeast growth, and 11 pairs that caused nonlethal growth defects (Fig. 4). On the *SMD1* side, the synthetic lethalities of *E18A*, *N37A*, *R88K*, and *R93A* with *SMD2* were highly correlated and contrasted with the comparatively benign mutational synergies of *Q35A* (Fig. 4). On the *SMD2* side, the synthetic lethalities and sicknesses were concentrated in *SMD2* alleles *R49A*, *N66A*, *E74A*, *R89A*, *R97K*, and *D99A* (Fig. 4). In contrast, we observed no synergies for *SMD2* alleles *N51A*, *K93A*, or *K106A*, and *SMD2* alleles *R57A* and *R63A* elicited *ts* or *cs* effects only in combination with *SMD1 N37A*.

SMD2 vs SMD1	E18A	Q35A	N37A	R88K	R93A
R49A	lethal	cs	lethal	lethal	lethal
N51A					
R57A			ts		
R63A			ts, cs		
N66A	lethal	ts	lethal	lethal	lethal
E74A	lethal		very sick	cs	
R89A			very sick		ts
K93A					
R97K	lethal	ts	lethal	lethal	lethal
D99A	lethal	ts	lethal	lethal	very sick
K106A					

SMB vs SMD1	E18A	Q35A	N37A	R88K	R93A
H40A			very sick		
N42A	sick		lethal	lethal	lethal
R88A	ts		lethal	very sick	very sick

SMD3 vs SMD1	E18A	Q35A	N37A	R88K	R93A
S39A			ts		
N41A	ts		lethal	lethal	very sick
R65A			lethal		ts

SMG vs SMD1	E18A	Q35A	N37A	R88K	R93A
F35A	sick		ts		
N37A	sick		lethal	lethal	lethal
R64A	sick		lethal	ts, cs	ts

SME vs SMD1	E18A	Q35A	N37A	R88K	R93A
F32A	ts		sick		
E33A					
F49A	ts		sick	ts, cs	
N51A	sick		lethal	ts, cs	ts
K83A	sick		lethal	very sick	sick

SMF vs SMD1	E18A	Q35A	N37A	R88K	R93A
K32A	lethal		lethal	lethal	lethal
F33A	sick		lethal	cs	cs
Y48A	ts		lethal	lethal	lethal
N50A	ts		ts		
R74K	lethal	ts	lethal	lethal	lethal

FIGURE 4. SmD1 mutations synergize with mutations in other Sm subunits. Synthetically lethal pairs of alleles are highlighted in red boxes. Other negative pairwise interactions are classified as sick or very sick (yellow boxes) or temperature sensitive (*ts*) or cold sensitive (*cs*) (light green boxes). Gray boxes denote lack of mutational synergy.

We then proceeded to test 95 pairwise combinations of the five *SMD1* alleles with benign mutations in SmB ($n = 3$), SmD3 ($n = 3$), SmG ($n = 3$), SmE ($n = 5$), and SmF ($n = 5$), focusing on their amino acids that comprise the RNA-binding triad. We thereby identified 25 cases of synthetic lethality that underscored the following themes (Fig. 4). First, the loss of SmD1 Gln35 (a component of the RNA binding triad) rarely elicited a synthetic phenotype (in only 1/19 pairs tested, which was no more severe than *ts* growth) (Fig. 4). Second, the loss of SmD1 Asn37 (the triad component that makes nucleobase-specific hydrogen bonds to the snRNA) consistently elicited the greatest number and severity of synthetic phenotypes with SmB, SmD3, SmG, SmE, and SmF mutations, i.e., 12 instances of synthetic lethality with at least two lethal combinations in every Sm subunit (Fig. 4). Third, mutation of SmD1 RNA-binding amino acids Arg88 (to Lys) and Arg93 (to Ala) also educed many synthetic lethalities with SmB, SmD3, SmG, SmE, and SmF mutations (six for *R88K*; five for *R93A*) as well as several nonlethal defects. Fourth, alanine substitution at SmD1 Glu18 was lethal only in combination with two mutations in SmF, yet caused synthetic sickness with a broad range of other Sm mutations. The all-against-all analysis highlights that permutations of the RNA-binding residues Glu18, Arg88, and Arg93 of SmD1 tend to have the greatest impact when combined with mutations in SmD2 and SmF (Fig. 4), which are the subunits located adjacent to SmD1 in the clockwise direction of the Sm ring (Supplemental Fig. S1A).

SmD2 mutational synergies within the Sm ring

Based on the results of the *SMD1*-against-*SMD2* synthetic array (Fig. 4) and the *SMD2* synergies with splicing factors (Fig. 1C), we chose six of the SmD2 mutations (*R49A*, *N66A*, *E74A*, *R89A*, *R97K*, *D99A*) and tested them in 114 pairwise combinations with our collection of mutations in SmB, SmD3, SmG, SmE, and SmF (Fig. 5). We noted 51 instances

SMB vs SMD2	R49A	N66A	E74A	R89A	R97K	D99A
H40A	very sick	very sick			very sick	very sick
N42A	lethal	lethal	sick	sick	lethal	lethal
R88A	lethal	lethal			lethal	lethal

SMD3 vs SMD2	R49A	N66A	E74A	R89A	R97K	D99A
S39A	cs	ts			sick	ts
N41A	lethal	lethal	sick		lethal	lethal
R65A	very sick	very sick			lethal	lethal

SMG vs SMD2	R49A	N66A	E74A	R89A	R97K	D99A
F35A		lethal	ts	ts	ts	ts
N37A	lethal	lethal	sick	ts	lethal	lethal
R64A	very sick	lethal	ts	sick	lethal	lethal

SME vs SMD2	R49A	N66A	E74A	R89A	R97K	D99A
F32A	cs	lethal		sick	lethal	lethal
E33A						
F49A		very sick			very sick	very sick
N51A	ts, cs	lethal	ts, cs	ts, cs	lethal	lethal
K83A	sick	lethal	ts, cs	sick	lethal	lethal

SMF vs SMD2	R49A	N66A	E74A	R89A	R97K	D99A
K32A	lethal	lethal	lethal	lethal	lethal	lethal
F33A	sick	lethal	ts	very sick	lethal	lethal
Y48A	lethal	lethal	ts	ts	lethal	lethal
N50A		lethal	ts	ts	sick	very sick
R74K	lethal	lethal	lethal	lethal	lethal	lethal

FIGURE 5. SmD2 mutational synergies within the Sm ring. Synthetically lethal pairs of alleles are highlighted in red boxes. Other negative pairwise interactions are classified as sick or very sick (yellow boxes) or temperature sensitive (*ts*) or cold sensitive (*cs*) (light green boxes). Gray boxes denote lack of mutational synergy.

of synthetic lethality, mostly involving mutations of SmD2 residues Asn66 ($n = 14$), Asp99 ($n = 13$), Arg97 ($n = 13$), and Arg49 ($n = 7$). In contrast, mutations of Glu74 and Arg89 elicited only two synthetic lethal interactions each (Fig. 5). The all-against-all analysis for SmD2 (Figs. 4A, 5) reveals that SmD2 mutations have the greatest number of synthetic lethalities when combined with mutations in SmF ($n = 20$) and SmD1 ($n = 16$), which are the subunits located on either side of SmD2 in the Sm ring (Supplemental Fig. S1A). SmD2 mutations educed fewer synthetic lethalities with changes in SmE ($n = 9$), SmG ($n = 8$), SmB ($n = 8$), or SmD3 ($n = 6$).

Specific yeast Sm ring mutations expose a requirement for assembly factor Brr1

The assembly of the human Sm ring around the Sm RNA site is an intricate and ordered process mediated by an ensemble of Gemin proteins and other factors, including the protein SMN (survival motor neuron) (Liu et al. 1997; Zhang et al. 2011; Grimm et al. 2013; Neuenkirchen et al. 2015). Mutations in the human *SMN1* gene are the cause of the disease spinal muscular atrophy (Lunn and Wang 2008; Chari et al. 2009). Less is known about the Sm assembly pathway in the simpler model organism *Saccharomyces cerevisiae*, beyond the fact that budding yeast has, in Brr1, a putative homolog of the key metazoan Sm assembly factor Gemin2 (Noble and Guthrie 1996; Liu et al. 1997; Kroiss et al. 2008), but no apparent homologs of the other Gemins or SMN. It is remarkable, indeed surprising, that Brr1 is inessential for vegetative growth of *S. cerevisiae* at temperatures ranging from 18°C–37°C (Supplemental Fig. S5). (A *brr1*Δ null strain displays an extreme cold-sensitive defect manifest as failure to thrive at ≤17°C [Noble and Guthrie 1996].) This suggests that the yeast Sm proteins are capable in vivo of self-assembling a closed ring structure around the Sm sites of U snRNAs without the agency of additional protein chaperones. (An alternative view, which we cannot exclude but consider less likely, is that yeast Sm ring assembly relies on essential proteins factors unique to budding yeast that are as yet unidentified.)

We reasoned that hypomorphic mutations in individual subunits of the yeast Sm ring, either at the RNA-binding site or the Sm–Sm subunit interfaces, might affect the putative self-assembly pathway and unmask a requirement for Brr1 to compensate for potentially weakened Sm protein–RNA or Sm protein–protein interactions. To put this idea to the test, we generated a series of seven *brr1*Δ *sm*Δ p[*CEN URA3 SM*] double-deletion strains in which the gene encoding Brr1 was deleted in tandem with deletions of the genes encoding each of the seven yeast Sm proteins. Sm function was supplied by a wild-type *SM* gene on a *CEN URA3* plasmid, thereby allowing tests of synthetic interactions of Sm mutations with *brr1*Δ via plasmid shuffle. We performed the synthetic genetic array with our collection of otherwise benign single missense mutations in the

SmF	SmE	SmG	SmD3	SmB	SmD1	SmD2
K32A	F20A	R23A	K9A	H40A	E18A	R49A
F33A	F32A	F35A	E13A	N42A	Q35A	N51A
Y48A	E33A	N37A	R30A	R52A	N37A	R57A
N50A	F49A	R64A	E35A	R80A	R88K	R63A
E58A	N51A		S39A	R88A	R93A	N66A
R74K	E59A		N41A			E74A
N77A	K83A		R65A			R89A
Y80A			K70A			K93A
			D76A			R97K
			N80A			D99A
			K85A			K106A
			K86A			

lethal
sick
ts
+++

FIGURE 6. Specific yeast Sm ring mutations expose a requirement for Brr1. The indicated Sm mutants were tested for *sm*Δ complementation in a *brr1*Δ genetic background. *brr1*Δ-lethal Sm mutations are highlighted in red boxes. *brr1*Δ-viable strains were tested for growth on YPD agar and classified as sick or very sick (yellow boxes) or temperature sensitive (*ts*) (light green boxes). Gray boxes denote wild-type growth.

SmF ($n = 8$), SmE ($n = 7$), SmG ($n = 4$), SmD3 ($n = 12$), SmB ($n = 5$), SmD1 ($n = 5$), and SmD2 ($n = 11$) proteins.

The salient findings were that specific mutations in the adjacent SmE, SmF, SmD2, and SmD1 subunits (but no mutations in the adjacent SmG, SmD3, and SmB subunits) were synthetically lethal with *brr1*Δ. The *brr1*Δ lethals (in red boxes in Fig. 6) were concentrated in SmD2 (*R49A*, *N66A*, *E74A*, *R97K*, *D99A*) and SmF (*K32A*, *F33A*, *R74K*), as were the Sm mutations that were synthetically very sick with *brr1*Δ, i.e., *SMD2 R89A* and *SMF E58A* and *N77A* (yellow boxes in Fig. 6). (Growth of the *SMD2* mutants in the *brr1*Δ background is shown in Supplemental Fig. S5.) *brr1*Δ lethals were less prevalent in the SmE (*K83A*) and SmD1 (*E18A*, *N37A*) subunits that abut SmF and SmD2, respectively. Sm mutations conferring a temperature-sensitive phenotype in the *brr1*Δ strain (in green boxes in Fig. 6) were distributed in SmF (*Y48A*, *N50A*), SmE (*F20A*, *F32A*, *N51A*), SmG (*N37A*, *R64A*), and SmB (*N42A*). SmD3 was conspicuous by virtue of the absence of any mutational synergies of 12 alanine mutations with *brr1*Δ (Fig. 6). Thus, there was a clear correlation between acquired essentiality of Brr1 and the angular position of the inciting mutations in the Sm ring.

Synthetic lethality with Sm mutations enables structure–function studies of yeast Brr1

We exploited the essentiality of Brr1 for growth of certain Sm mutants to initiate a structure–function analysis of the 341-amino acid Brr1 protein, guided by its N-terminal and C-terminal sequence similarity to the human and *Drosophila* Gemin2 proteins (Fig. 7). To address the contributions of the N-terminal segment to Brr1 function, we serially deleted 23, 48, 77, or 136 amino acids. The wild-type and *BRR1-N*Δ alleles were placed on *CEN LEU2* plasmids under the control of the native *BRR1* promoter and cotransformed with a *CEN*

HIS3 SMF-F33A plasmid into a *brr1*Δ *smf*Δ p[*CEN URA3 SMF*] strain. His^+ Leu^+ transformants were streaked on agar medium containing FOA to select against the plasmid bearing wild-type *SMF*. If the plasmid-encoded Brr1 protein is biologically active, then it will allow the growth of cells expressing *SMF-F33A* on FOA. Failure to recover FOA-resistant survivors signifies that a mutated Brr1 is nonfunctional. The wild-type *BRR1* plasmid passed the *brr1*Δ *SMF-F33A* complementation test and the FOA-resistant strains grew on YPD agar at all temperatures tested (Fig. 7). *BRR1-NΔ23* also complemented *brr1*Δ *SMF-F33A*; the *BRR1-NΔ23 SMF-F33A* cells grew as well as *BRR1 SMF-F33A* cells at 18°C–30°C, but were sick at 37°C (Fig. 7). In contrast, the *NΔ48*, *NΔ77*, and *NΔ136* alleles failed to complement *brr1*Δ *SMF-F33A*. We conclude that the N-terminal segment from amino acids 24–47 is essential for Brr1 function in the *SMF-F33A* background. Similar results were obtained when we tested the same *BRR1* alleles for *brr1*Δ *SME-K83A* complementation (Supplemental Fig. S6), i.e., *BRR1-NΔ23 SME-K83A* cells grew well at 20°C–30°C but slowly at 37°C, whereas the *NΔ77* and *NΔ136* alleles failed to complement *brr1*Δ *SME-K83A*. The *NΔ48* mutant gave rise to FOA survivors after 7–10 d but the *BRR1-NΔ48 SME-K83A* cells failed to grow on YPD agar at any temperature.

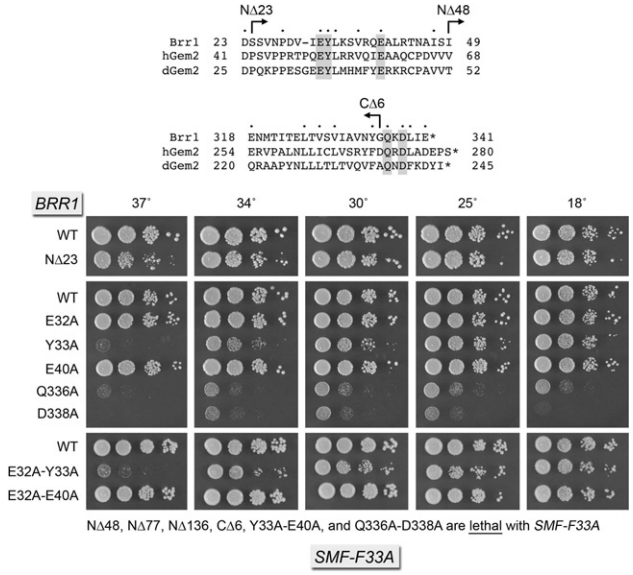

FIGURE 7. Structure–function analysis of yeast Brr1 by complementation of *brr1*Δ *SMF-F33A*. (*Top* panel) Alignment of the primary structures of the near-N-terminal and C-terminal segments of *S. cerevisiae* Brr1, human Gemin2 (hGem2), and *Drosophila* Gemin2 (dGem2). Positions of side chain identity/similarity in all three proteins are indicated by (•) *above* the yeast sequence. *Forward* and *reverse* arrowheads indicate the boundaries of the N-terminal and C-terminal truncations of yeast Brr1. (*Bottom* panel) The wild-type and mutated *BRR1* alleles were tested for *brr1*Δ *SMF-F33A* complementation by plasmid shuffle. The viable FOA-resistant *SMF-F33A* strains bearing the indicated *BRR1* alleles were spot-tested for growth on YPD agar at the temperatures specified.

Alignment of Brr1 and Gemin2 highlights conservation within the C-terminal Brr1 hexapeptide ^{336}QKDLIE^{341} (Fig. 7). A truncated *BRR1-CΔ6* allele encoding Brr1-(1–335) failed both *brr1*Δ *SMF-F33A* complementation (Fig. 7) and *brr1*Δ *SME-K83A* complementation (Supplemental Fig. S6), signifying that the C-terminal hexapeptide is essential for Brr1 activity in these genetic backgrounds.

Alanine mutations of the essential N and C segments of yeast Brr1

We conducted an alanine scan of Brr1 N-terminal residues Glu32, Tyr33, and Glu40 and C-terminal residues Gln336 and Asp338 that are conserved in human and *Drosophila* Gemin2. Whereas the *BRR1 E32A* and *E40A* alleles were fully functional in both *brr1*Δ *SMF-F33A* complementation (Fig. 7) and *brr1*Δ *SME-K83A* complementation (Supplemental Fig. S6), the *Y33A*, *Q336A*, and *D338A* alleles were functional hypomorphs. *Y33A* was temperature sensitive in the *SMF-F33A* strain, whereas *Q336A* and *D338A* were very sick with *SMF-F33A* under all conditions tested (Fig. 7). Similar growth phenotypes were seen for *Y33A*, *Q336A*, and *D338A* in the *SME-K83A* background (Supplemental Fig. S6).

To evaluate whether any of these neighboring Brr1 amino acids might overlap functionally, we tested various double-alanine pairs. The *E32A-E40A* double-mutant was fully active in *brr1*Δ *SMF-F33A* and *brr1*Δ *SME-K83A* complementation. The *E32A-Y33A* double mutant displayed the same temperature-sensitive phenotype as the *Y33A* single mutant in the *SMF-F33A* strain (Fig. 7); *E32A-Y33A* had an intermediate phenotype in the *SME-K83A* background, growing slightly better than *Y33A* at 37°C but worse than *Y33A* at 20°C (Supplemental Fig. S6). The instructive findings were that the *Y33A-E40A* and *Q336A-D338A* double mutants were both lethal in the *SMF-F33A* and *SME-K83A* genetic backgrounds, signifying functional overlap of the conserved Tyr33-Glu40 and Gln336-Asp338 amino acid pairs.

DISCUSSION

The seven subunits of the SmF–E–G–D3–B–D1–D2 ring recognize seven consecutive nucleotides in the uridine-rich Sm sites of the U1, U2, U4, and U5 snRNAs. Given the conservation from yeast to humans of the core Sm ring structure and the shared principle of RNA recognition via an amino acid triad present in each Sm subunit, one might have expected the Sm protein–RNA complex to be functionally acutely sensitive to perturbations of the protein–RNA interface and/or Sm–Sm subunit interface. This is apparently not the case in budding yeast, insofar as: (i) genetic analyses showed that whereas deletion of the AUUUUUU Sm site of U5 snRNA was lethal, replacing any one of the seven Sm nucleotides with the three other nucleobases was tolerated in 18 of 21 cases (Jones and Guthrie 1990); and (ii) our comprehensive structure-guided alanine scan of all seven yeast Sm

proteins revealed that only 2 of 54 alanine mutations were lethal (Supplemental Fig. S1B).

The present study is the third (and closing) installment of our structure–function and synthetic genetics analysis of the yeast Sm proteins, which was conducted stepwise for the SmD3-B, SmF-E-G, and now SmD1-D2 subcomplexes of the ring. Four broad themes emerged. First, the fact that lethal single-alanine mutations were confined to the RNA-binding sites of SmD1 (Arg88) and SmD2 (Arg97) highlights the unique importance of their π-cation interactions with the sixth and seventh nucleobases of the Sm RNA site, respectively. This conclusion is fortified by the finding that both arginines can be replaced functionally by lysine. Alanine mutation of SmF Arg74 caused a severe growth defect, which was reversed by lysine (Schwer et al. 2016), signifying that the π-cation stack on the first nucleobase of the Sm RNA site is important too. In the same vein, alanine mutation of SmD2 His64 (which with Arg97 can form a π-cation sandwich on its Sm uridine nucleobase) also caused a severe growth defect. What remains unresolved via Sm protein genetics is whether the lethality or severe growth defects caused by loss of the SmD1, SmD2, or SmF arginines or the SmD2 histidine reflect dysfunction of all of the Sm ring-containing snRNPs or of one snRNP in particular.

Second, the lack of effect of the majority of the Sm single-alanine mutations on yeast growth reflects genetic buffering by other Sm subunits picking up the slack. All-against-all testing of 406 pairwise combinations of benign mutations of the seven Sm subunits has unveiled a wide network of 137 intersubunit synthetic lethalities. These results signify that five of seven intact RNA binding sites in the Sm ring do not suffice for in vivo function.

Third, the aggregate synthetic array results here for SmD2 and SmD1 and previously for the five other Sm subunits (Schwer and Shuman 2015; Schwer et al. 2016) fortify the theme that the function or structural integrity of the yeast U2 snRNP is especially sensitive to otherwise benign perturbations of the RNA-binding or subunit interfaces of the Sm ring when either component of the Lea1•Msl1 subassembly of the U2 snRNP is missing. Supplemental Figure S4 lists the 24 mutations in the yeast Sm subunits that are synthetically lethal with *msl1*Δ, which are distributed fairly evenly across the seven Sm proteins (3– 4 per Sm subunit).

Finally, we deployed our extensive Sm mutant collection to illuminate the function of the yeast Sm assembly factor Brr1 and its relationship to the metazoan Sm assembly factor Gemin2. Brr1 being inessential for vegetative growth of *S. cerevisiae* implies that the yeast Sm ring can assemble on snRNAs without the aid of a Gemin2-type chaperone. Our new findings that certain mutations in the adjacent SmE, SmF, SmD2, and SmD1 subunits (but none in the adjacent SmG, SmD3, and SmB subunits) are synthetically lethal with *brr1*Δ empowers budding yeast as a model genetic system to study chaperoned Sm assembly. We conclude that specific perturbations of the SmE–F–D2–D1 ring segment affect self-assembly and unmask a requirement for Brr1 to compensate. The subunit specificity of the *brr1*Δ synthetic lethalities accords with the elegant biochemical and structural studies of human and *Drosophila* Gemin2 and their interactions with Sm subunits (Zhang et al. 2011; Grimm et al. 2013). Gemin2 wraps around the perimeter of a C-shaped SmD1–D2–F–E–G assembly intermediate that lacks SmD3-B. Gemin2 is composed of: (i) a C-terminal 180-amino acid all-α-helical domain that packs against the SmD2 and SmD1 subunits; (ii) a near-N-terminal α1 helix that packs against SmE and SmF; and (iii) an extended loop that connects the N and C modules by draping loosely over the central SmD2 and SmF subunits of the Sm crescent. Gemin2 makes little or no contact with SmG. Thus, the observed gradient of *brr1*Δ lethalities is concentrated in the very Sm subunits with which Gemin2 is most intimately engaged.

Using complementation of synthetic *brr1*Δ lethality in two Sm mutant backgrounds as an in vivo assay of Brr1 activity, we showed that the near-N-terminal segment of Brr1 from amino acids 24–47 is essential. This Brr1 segment corresponds to the N-terminal α1 helix of human and *Drosophila* Gemin2. Alanine scanning of conserved amino acids within this α-helix pinpoints the Tyr33-Glu40 pair as essential for Brr1 function. Figure 8A shows that the equivalent Tyr52-Glu59 pair in human Gemin2 emanates from the Sm-facing side of the α1 helix and that the tyrosine and glutamate side chains together make hydrogen bonds to a conserved SmF asparagine located at the start of the SmF α1 helix (Asn6 in human SmF; Asn14 in yeast SmF). The overlapping atomic contacts to the same SmF asparagine rationalize the functional redundancy imputed genetically to Brr1 Tyr33 and Glu40, whereby a *Y33A-E40A* double mutant was lethal but the single *Y33A* and *E40A* mutants were *ts* and benign, respectively. The Gemin2 structure also clarifies why the Brr1 *E32A* mutation had no impact, per se or in combination with *E40A*, i.e., because the equivalent Glu51 side chain in Gemin2 projects from the opposite solvent exposed face of the α1 helix and makes no Sm contacts (Fig. 8A).

We demonstrated that the C-terminal hexapeptide of yeast Brr1 is essential for its function, via the presence of conserved residues Gln336 and Asp338. The *Drosophila* Gemin2 structure nicely illuminates the basis for their importance by virtue of their participation in a network of atomic contacts to the β4 strand of the SmD2 protein (Fig. 8B). Gemin2 Gln238 (Brr1 Gln336) makes a bidentate hydrogen bond to main-chain amide nitrogen and carbonyl oxygen atoms of SmD2 and also, along with Gemin2 Asp240 (Brr1 Asp338), coordinates a conserved arginine (Arg201 in Gemin2; Arg278 in Brr1) that makes a salt bridge to a conserved carboxylate side chain in SmD2 (Fig. 8B).

In summary, we have: (i) advanced the genetics of the yeast Sm ring to a level commensurate with the detailed structural biology of the Sm ring; (ii) placed yeast Brr1 firmly in a genetic pathway of Sm assembly; and (iii) provided the enabling

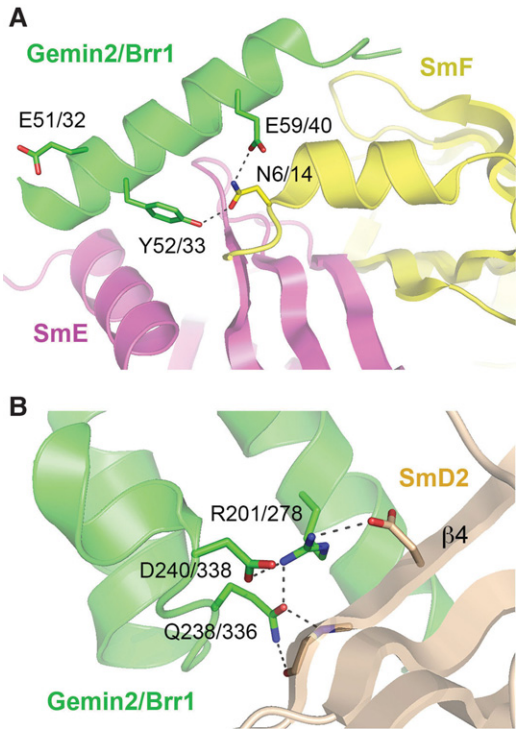

FIGURE 8. Gemin2 structures rationalize the importance of Brr1 N- and C-terminal motifs. (*A*) Interaction of the N-terminal α-helix of human Gemin2 (Brr1 homolog; colored green) with the SmF subunit (colored yellow) of the penta-Sm assembly intermediate (from pdb 3S6N; Zhang et al. 2011). hGem2 Glu51, Tyr52, and Glu59 counterparts of the conserved Brr1 Glu32, Tyr33, and Glu40 residues that were subjected to alanine scanning are shown as stick models. Hydrogen bonds from Tyr52/33 and Glu59/40 to a conserved N-terminal asparagine of SmF are denoted by dashed lines. (*B*) Interaction of the C-terminal module of *Drosophila* Gemin2 (green) with the β4 strand of the SmD2 subunit (beige) of a penta-Sm assembly intermediate (from pdb 4V98, Grimm et al. 2013). dGem2 Gln238 and Asp240 are the counterparts of the conserved C-terminal Brr1 Gln336 and Asp338 residues that were subjected to alanine scanning.

tools for structure–function analysis of Brr1 and its relationship to metazoan Gemin2.

MATERIALS AND METHODS

Yeast expression plasmids and mutants

A series of expression plasmids for the *SMD1*, *SMD2*, and *BRR1* genes were generated by PCR amplification of DNA segments from *S. cerevisiae* DNA with oligonucleotide primers that introduced restriction sites for cloning into pRS316 (*URA3 CEN*), pRS413 (*HIS3 CEN*), and pRS415 (*LEU2 CEN*) vectors. Missense and deletion mutations were introduced by two-stage PCR overlap extension with mutagenic primers. PCR overlap extension was also used to remove the 96-bp intron from the *SMD2* gene. The PCR products were digested and then inserted into the centromeric plasmids. All genes in the resulting plasmids were sequenced completely to confirm that no unwanted changes were acquired during amplification and cloning. We thereby generated p316-SMD1 and p413-SMD1, wherein the 441-bp *SMD1* ORF is flanked by 400-bp and 250-bp of upstream and downstream genomic sequence. The expression plasmids for the *SMD2* gene contain the 333-bp *SMD2* ORF plus 400-bp and 250-bp of upstream and downstream flanking sequences. Mutations of *SMD1* and *SMD2* were introduced into the pRS413- and pRS415-based expression plasmids, respectively. The pRS415-based expression plasmids for *BRR1* contain the 1026-bp *BRR1* ORF flanked by 720-bp and 330-bp of upstream and downstream genomic sequences. We also generated 11 p316-SM/SM plasmids (*URA3 CEN*) carrying pairwise combinations of *SMD1* (nucleotides −400 to +691) with *SMD2* (nucleotides −400 to +583), *SMG* (nucleotides −470 to +720), *SME* (nucleotides −148 to +560), *SMF* (nucleotides −205 to +543), *SMB* (nucleotides −500 to +875), and *SMD3* (nucleotides −445 to +552) and pairwise combination of *SMD2* with *SMG*, *SME*, *SMF*, *SMB*, and *SMD3*.

Yeast strains and tests of function in vivo

All strains used are haploid progeny (*his3*Δ *leu2*Δ *ura3*Δ) of BY4743, a derivative of S288C. To develop plasmid shuffle assays to test the effects of *SMD1 and SMD2* mutations, we first generated *smd1*Δ p[*URA3 CEN SMD1*] and *smd2*Δ p[*URA3 CEN SMD2*] haploids by sporulation and dissection of heterozygous *SMD1 smd1*Δ::*kanMX* and *SMD2 smd2*Δ::*kanMX* diploids that had been transfected with pRS316-based *SMD1* or *SMD2* expression plasmids. *smd1*Δ p[*URA3 CEN SMD1*] and *smd2*Δ p[*URA3 CEN SMD2*] cells were resistant to G418 and unable to grow on medium containing 0.75 mg/mL 5-fluoroorotic acid (FOA). (Note that the *smd2*Δ p[*URA3 CEN SMD2*] cells grew as well as *SMD2* haploids signifying that removal of the intron in the plasmid-borne *SMD2* gene elicited no discernible effect on cell growth.) To assay the function of, for example, wild-type and mutated *SMD1* alleles, *smd1*Δ p[*URA3 CEN SMD1*] cells were transfected with pRS413-based *SMD1* expression plasmids. Individual His^+ transformants were selected and streaked on agar medium containing FOA. The plates were incubated at 20°C, 30°C, and 37°C and mutants that failed to form macroscopic colonies at any temperature after 8 d were deemed lethal. Individual FOA-resistant colonies with viable *SM* alleles were grown to mid-log phase in YPD broth and adjusted to the same A_{600} values. Aliquots (3 μL) of serial 10-fold dilutions were spotted on YPD agar plates, which were then incubated at temperatures ranging from 18°C or 20°C to 37°C. We also developed plasmid shuffle assays to test the effects of *SMD1* and *SMD2* mutations in *nam8*Δ, *mud1*Δ, *mud2*Δ, *tgs1*Δ, *cbc2-Y24A*, *lea1*Δ, and *msl1*Δ genetic backgrounds, using standard genetic manipulations of mating, sporulation, and dissection. Similar strategies were also used to generate the strains for investigating genetic interactions between *BRR1* and each of the genes encoding the subunits of the Sm complex. The strains and plasmids for *SMB, SMD3, SMG, SME*, and *SMF* genetics were described previously (Schwer and Shuman 2015; Schwer et al. 2016).

Tests of mutational synergy with other Sm subunits

Haploid strains in which pairs of *sm*Δ alleles are complemented by the corresponding pRS316-SM/SM plasmids were generated by pairwise crossing of *sm*Δ pRS316-SM haploids of the opposite mating type. The heterozygous diploids were plated to FOA agar to select against the *URA3 CEN SM* plasmids and subsequently transfected with the appropriate p316-SM/SM plasmids. Ura^+ transformants were

selected and subjected to sporulation and dissection. We thereby generated strains *smd1Δ::kanMX smd2Δ::natMX* p[*URA3 CEN SMD1 SMD2*], *smd1Δ::kanMX smbΔ::natMX* p[*URA3 CEN SMD1 SMB*], *smd1Δ::kanMX smd3Δ::hygMX* p[*URA3 CEN SMD1 SMD3*], *smd1Δ::kanMX smgΔ::hygMX* p[*URA3 CEN SMD1 SMG*], *smd1Δ::kanMX smeΔ::natMX* p[*URA3 CEN SMD1 SME*], *smd1Δ::kanMX smfΔ::natMX* p[*URA3 CEN SMD1 SMF*], *smd2Δ::kanMX smbΔ::natMX* p[*URA3 CEN SMD2 SMB*], *smd2Δ::kanMX smd3Δ::hygMX* p[*URA3 CEN SMD2 SMD3*], *smd2Δ::kanMX smgΔ::hygMX* p[*URA3 CEN SMD2 SMG*] *smd2Δ::kanMX smeΔ::natMX* p[*URA3 CEN SMD2 SME*], and *smd2Δ::kanMX smfΔ::natMX* p[*URA3 CEN SMD2 SMF*] that failed to grow on FOA medium unless they had been co-transformed with *CEN HIS3* plus *CEN LEU2* plasmids harboring the corresponding *SM* genes. The function of mutated *SM* alleles in various combinations was assessed as described above with the exception that counter-selection on FOA was carried out at 30°C only and double mutants were deemed lethal if they failed to grow after 8 d of incubation at 30°C.

SUPPLEMENTAL MATERIAL

Supplemental material is available for this article.

ACKNOWLEDGMENTS

This work was supported by National Institutes of Health grants GM52470 (S.S. and B.S.) and GM102961 (B.S.).

Received November 3, 2016; accepted December 12, 2016.

REFERENCES

Bordonné R. 2000. Functional characterization of nuclear localization signals in yeast Sm proteins. *Mol Cell Biol* **20:** 7943–7954.

Chari A, Paknia E, Fischer U. 2009. The role of RNP biogenesis in spinal muscular atrophy. *Curr Opin Cell Biol* **21:** 387–393.

Galej WP, Wilkinson ME, Fica SM, Oubridge C, Newman AJ, Nagai K. 2016. Cryo-EM structure of the spliceosome immediately after branching. *Nature* **537:** 197–201.

Girard C, Mouaikel J, Neel H, Bertrand E, Bordonné R. 2004. Nuclear localization properties of a conserved protuberance in the Sm core complex. *Exp Cell Res* **299:** 199–208.

Grimm C, Chari A, Pelz JP, Kuper J, Kisker C, Diederichs K, Stark H, Schindelin H, Fischer U. 2013. Structural basis of assembly chaperon-mediated snRNP formation. *Mol Cell* **49:** 692–703.

Hang J, Wan R, Yan C, Shi Y. 2015. Structural basis of pre-mRNA splicing. *Science* **349:** 1191–1198.

Hausmann S, Zheng S, Costanzo M, Brost RL, Garcin D, Boone C, Shuman S, Schwer B. 2008. Genetic and biochemical analysis of yeast and human cap trimethylguanosine synthase: functional overlap of TMG caps, snRNP components, pre-mRNA splicing factors, and RNA decay pathways. *J Biol Chem* **283:** 31706–31718.

Jones MH, Guthrie C. 1990. Unexpected flexibility in an evolutionarily conserved protein-RNA interaction: genetic analysis of the Sm binding site. *EMBO J* **9:** 2555–2561.

Kambach C, Walke S, Yound R, Avis JM, de la Fortelle E, Raker VA, Lührmann R, Li J, Nagai K. 1999. Crystal structures of two Sm protein complexes and their implications for the assembly of the spliceosomal snRNPs. *Cell* **96:** 375–387.

Kondo Y, Oubridge C, van Roon AM, Nagai K. 2015. Crystal structure of human U1 snRNP, a small nuclear ribonucleoprotein particle, reveals the mechanism of 5′ splice site recognition. *eLife* **4:** e04986.

Kroiss M, Schultz J, Wiesner J, Chari A, Sickmann A, Fischer U. 2008. Evolution of an RNA assembly system: a minimal SMN complex facilitates formation of UsnRNPs in *Drosophila melanogaster*. *Proc Natl Acad Sci* **105:** 10045–10050.

Li J, Leung AK, Kondo Y, Oubridge C, Nagai K. 2016. Re-refinement of the spliceosomal U4 snRNP core-domain structure. *Acta Crystallogr D Struct Biol* **72:** 131–146.

Liu Q, Fischer U, Wang F, Dreyfuss G. 1997. The spinal muscular atrophy gene product, SMN, and its associated protein SIP1 are in a complex with spliceosomal snRNP proteins. *Cell* **90:** 1013–1021.

Lunn MR, Wang CH. 2008. Spinal muscular atrophy. *Lancet* **371:** 2120–2133.

Mouaikel J, Verheggen C, Bertrand E, Tazi J, Bordonné R. 2002. Hypermethylation of the cap structure of both yeast snRNAs and snoRNAs requires a conserved methyltransferase that is localized to the nucleolus. *Mol Cell* **9:** 891–901.

Neuenkirchen N, Englbrecht C, Ohmer J, Ziegenhals T, Chari A, Fischer U. 2015. Reconstitution of the human U snRNP assembly machinery reveals stepwise Sm protein organization. *EMBO J* **34:** 1925–1941.

Nguyen THD, Galej WP, Bai X, Savva CG, Newman AJ, Scheres SHW, Nagai K. 2015. The architecture of the spliceosomal U4/U6.U5 tri-snRNP. *Nature* **523:** 47–52.

Noble SM, Guthrie C. 1996. Transcriptional pulse-chase analysis reveals a role for a novel snRNP-associated protein in the manufacture of spliceosomal snRNPs. *EMBO J* **15:** 4368–4379.

Qiu ZR, Chico L, Chang J, Shuman S, Schwer B. 2012. Genetic interactions of hypomorphic mutations in the m^7G cap binding pocket of yeast nuclear cap binding complex: an essential role for Cbc2 in meiosis via splicing of *MER3* pre-mRNA. *RNA* **18:** 1996–2011.

Schwer B, Shuman S. 2015. Structure-function analysis and genetic interactions of the Yhc1, SmD3, SmB, and Snp1 subunits of yeast U1 snRNP and genetic interactions of SmD3 with U2 snRNP subunit Lea1. *RNA* **21:** 1173–1186.

Schwer B, Kruchten J, Shuman S. 2016. Structure-function analysis and genetic interactions of the SmG, SmE, and SmF subunits of the yeast Sm protein ring. *RNA* **22:** 1320–1328.

van der Feltz C, Anthony K, Brilot A, Pomeranz Krummel DA. 2012. Architecture of the spliceosome. *Biochemistry* **51:** 3321–3333.

Wan R, Yan C, Bai R, Wang L, Huang M, Wong CL, Shi Y. 2016a. The 3.8 Å structure of the U4/U6.U5 tri-snRNP: insights into spliceosome assembly and catalysis. *Science* **351:** 446–475.

Wan R, Yan C, Bai R, Huang G, Shi Y. 2016b. Structure of a yeast catalytic step I spliceosome at 3.4 Å resolution. *Science* **353:** 895–904.

Weber G, Trowitzsch S, Kastner B, Lührmann R, Wahl MC. 2010. Functional organization of the Sm core in the crystal structure of human U1 snRNP. *EMBO J* **29:** 4172–4184.

Yan C, Wan R, Bai R, Huang G, Shi Y. 2016. Structure of a yeast catalytically activated spliceosome at 3.5 Å resolution. *Science* **353:** 904–911.

Zhang R, So BR, Li P, Yong J, Glisovic T, Wan L, Dreyfuss G. 2011. Structure of a key intermediate of the SMN complex reveals Gemin2's crucial function in snRNP assembly. *Cell* **146:** 384–395.